https://doi.org/10.15407/ujpe66.8.664

V. KOZUBOVSKY, YU. BILAK

Uzhgorod National University
(89a, Zankovetskoi Str., Uzhgorod 88000, Ukraine;
e-mail: yubill76@gmail.com, yuriy.bilak@uzhnu.edu.ua)

PHASE METHODS IN ABSORPTION SPECTROSCOPY

The analysis of the air gas composition is a challenging task because the well-being and health of the people depend on its quality. Most methods to analyze the gaseous medium are not perfect, and the necessary sensitivity, selectivity, and accuracy are often lack. The article analyzes a possibility to optimize the selectivity and accuracy of interferometric (refractometric) gas analysis devices. The main idea of the work is to demonstrate the possibility of a transition from the direct measurement of the ratio between the light flux intensities to the measurement of frequency shifts and radiation frequency, which significantly increases the accuracy and sensitivity of the measurements. In order to enhance the selectivity of the analysis, measurements are proposed to be done in the area of the anomalous dispersion of the analyzed gas component. The presence of the phase component of the useful signal, which is several orders of magnitude larger than the amplitude component in the region of the anomalous dispersion of the analyte and linearly depends on the concentration, allows the measurements to be made in a wide interval of analyte concentrations. All that opens new opportunities for interferometric methods of gas analysis.

K e y w o r d s: interferometer, anomalous dispersion, ring gas laser, gas analyzer, absorption spectroscopy.

1. Introduction

Absorption and interferometric (refractometric) methods are most often used to analyze the gas composition of the medium. One of the most widespread interferometric methods for studying the gas composition is the application of a Jamin interferometer. Here, the reference cuvette is filled with a reference gas, and the analyzed gas (more precisely, a mixture of the analyzed and reference gases) is passed through the working cuvette. The concentration of the analyzed gas in the mixture is determined by measuring the ratio between the intensity of light that is absorbed in the analyzed sample in the working cuvette, $\Delta\Phi$, and the intensity of the light flux Φ_0 that passes through the reference cuvette filled with the reference gas. As a rule, the measurement accuracy of the quantity $\Delta\Phi/\Phi_0$ does not exceed 10^{-3} in ordinary photometers. This method is neither highly accurate nor selective, i.e. one has to know in advance what gases are measured.

When using the absorption methods of analysis, the ratio between the intensities of the light flux $\Delta\Phi$ at the wavelength absorbed by the analyzed gas (the working channel) and the light flux Φ_0 that passed through the analyzed gas without absorption (at the reference wavelength) is measured, as a rule. Alternatively, the working and reference cuvettes are also used as in the previous example. Then, the ratio $\Delta\Phi/\Phi_0$ is measured, i.e. there arises a similar problem, a low measurement accuracy of photometric

quantities. This circumstance hinders the progress in the enhancement of the metrological parameters of absorption analytical instruments.

Various methods of correlation spectroscopy [1, 2] are used to increase the accuracy and selectivity of the measurements. However, those methods are rather difficult in technical implementation. Mechanical correlation masks must exactly reproduce the spectrum of the analyzed gas [1], and in the case of gas filtration, filters are used in the form of gas cuvettes filled with the measured (interfering) gas [2]. At the same time, the progress in interferometric (phase) measurements is substantial [3]. In this regard, it is of interest to change from the measurements of photometric quantities to the measurements of the phase shift and the frequency of radiation when it is absorbed by the analyte.

2. Substantiation of the Method

The absorption coefficient is known to be the imaginary part of the complex refractive index,

$$n' = n - ik, \tag{1}$$

where n is the real part of the refractive index (for gases, it is close to unity beyond the absorption bands), k is the imaginary part of the refractive index that is responsible for the damping of the electromagnetic wave ($k = K\lambda_0/4$), and K is the absorption coefficient.

Near the absorption line with the frequency ω_0 and the uniform width γ, the parameters k and n can be written in the form [4]

$$k = \frac{Ne^2}{8m\varepsilon_0}\frac{\gamma}{(\omega_0-\omega)^2+(\gamma/2)^2}, \tag{2}$$

$$n = 1 + \frac{Ne^2}{4m\varepsilon_0}\frac{\omega_0-\omega}{(\omega_0-\omega)^2+(\gamma/2)^2}, \tag{3}$$

where e is the magnitude of oscillator's electric charge, N the number of oscillators per unit volume, ε_0 the electric constant, and m oscillator's mass. In the case of a line with the Doppler broadening, expression (2) will be more complicated [5].

As one can see, the expressions for k and n are very similar and they include the same variables and constants. Considerable changes with k and n take place near the absorption line ($\omega \to \omega_0$). The characters of those changes are different. The dependence $k(\omega)$ reproduces the contour of the absorption line, whereas $n(\omega)$ has a dispersion character and is the first derivative of the absorption line contour.

As is known, the relationship between the quantities k and n makes it possible, using the Fourier transformation, to reproduce the absorption spectrum of the analyzed gas according to the interferogram obtained by scanning the optical length of one of the arms of a two-beam interferometer [6, 7].

The choice of that or another method to analyze the gas components depends on the quantities n and k in the specific spectral interval, as well as on the difference between themfor the analyzed gas and the interfering components. If the light flux with the intensity I passes through a cuvette of the length L located in the interferometer and filled with a gas with the concentration X, the absorption index of which is equal to K, and the refractive index n differs from the refractive index of air by Δn, then, the change ΔI in the light flux that falls onto the photodetector mounted behind the interferometer looks like (in the first approximation) [6]

$$\Delta I/I = (XKL + 2\pi L\Delta nX/\lambda). \tag{4}$$

Thus, expression (4) allows making a choice between the phaexceed a change of the optical density. In the visible spectral interval, which is the most convenient for optical measurements, the absorption coefficient of the main gas components that pollute the atmosphere equals almost zero. Therefore, interferometric gas analysis devices are applied in this case.

However, devices that combine the advantages of the phase and adsorption methods of analysis can be created. Let us consider some specific examples.

3. Absorption Analyzer with Interferometric Registration of Light Energy Absorbed by the Analyzed Gas

Let us first consider a possibility to create an absorption analyzer with the interferometric registration of the light energy absorbed by the analyzed gas. In this case, the gas is heated up. However, we are interested in the accompanying change in the gas refractive index. Then, the phase shift emerging in the interferometer arm with the working cuvette equals [8]

$$\Delta\Phi = \frac{4\pi KELD}{J\xi\lambda}\frac{dn}{dt}, \tag{5}$$

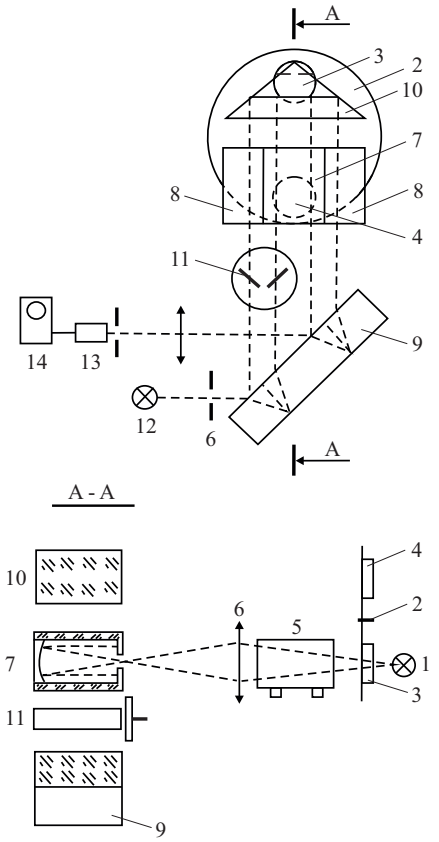

Fig. 1. Experimental analyzer of elegas SF_6

where E is the two-dimensional energy density, L the cuvette length, K the absorption coefficient, ξ the thermal conductivity, $J = 4.184$ J/cal, $D = \xi/(pC_p)$ is the mass density, and C_p the specific heat.

As an example, let us consider a possibility to use this method to analyze CO_2 at a wavelength of 4.2 μm (the parameters of the corresponding absorption bands are well studied). For CO_2, $K = 10$ (cm atm)$^{-1}$, $\rho = 11.84 \times 10^{-3}$ g/cm^3, $\xi = 0.34 \times 10^{-4}$ cal/(cm K), and $C_p = 0.196$ cal/(g K).

Let us be able to register $\Delta I/I = \Delta\Phi \sim 10^{-4}$ [Eq. (4)]. Then, in order to register the phase shift, the two-dimensional energy density must be $E > 2.56 \times 10^{-8}$ W. If the modulation frequency is 1 Hz and the illuminated area equals 1 mm^2 (photoresistor FUO614-5), we obtain that the minimum detectable light flux is $\Phi = 2.56 \times 10^{-10}$ W. This value is lower than those for the most sensitive IR photoresistors. For this reason, it is expectable that the application of the phase methods for the registration of light fluxes absorbed by the analyzed gas will allow the sensitivity of absorption analyzers and, of course, their selectivity to be substantially enhanced.

In Fig. 1, *a*, the schematic diagram of an experimental analyzer with a phase-sensitive sensor to analyze the sulfur hexafluoride elegas (SF_6) is shown [9]. The analyzer operates as follows. Radiation from source *1* is directed through light filter *3* (the maximum transmittance at 947 cm^{-1}, the working spectral region) or light filter *4*, which extracts a reference frequency of 1050 cm^{-1}. The light filters are alternately introduced into the light flux by modulator *2*. Then, radiation enters working cuvette *5*, through which the SF_6 mixture with a concentration of about 0.01 vol% is pumped. Afterward, the light flux is focused by lens *6* into reference cuvette *7* of the interferometer. The walls of the cuvette are covered with a light-reflective layer. Cuvette *7* is filled with a mixture of the analyzed gas (SF_6) and a solvent gas, which has low thermal conductivity and heat capacity (Xe, Ar). The concentration of SF_6 (1 vol% in Ar) was chosen so that radiation was completely absorbed in cuvette *7* during 1–2 passes. As a result of radiation absorption, the gas is heated up and, accordingly, the refractive index changes. However, this occurs only in the case of radiation with the wavelength corresponding to the center of the absorption line (the working wavelength). For the reference wavelength, the analyzed gas is transparent, and its heating is possible only due to a non-selective absorption of radiation by the walls and windows of the cuvette (the background signal). Those changes of the refractive indices n_p and n_0 are detected using a Jamin interferometer. In this interferometer, radiation from source *12* (a lamp OP6-3) is divided by means of plate *9* into two fluxes. One of them passes through reference cuvette *7*, and the other through comparison cuvette *8* filled with dilute gas (Ar). Those fluxes are reflected from rotary prism *10*, re-pass through their cuvettes, and get mixed at light-separating plate *9*. With the help of lens *6*, the resulting interference pattern is focused on photodetector *13* (FEP-86). Compensator *11* maintains a constant position of the achromatic band with respect to the FEP-86 photocathode (a constant position of its operating point is provided). In front of the FEP, a diaphragm 20 μm in width is installed. It extracts the center of the achromatic band wing,

which provides the maximum sensitivity of the analysis. A short-term shift of the interference pattern is detected by the FEP and registered using storage oscilloscope *14* (C1-31). Provided the indicated parameters of the experimental equipment, the variable signal measured by the FEP at its nominal supply and a load resistance of 1 MΩ corresponded to a voltage of 1 V. The obtained signal-to-noise ratio was 1200.

So one can see that interferometric infrared sensors can successfully compete with optical-acoustic receivers possessing approximately the same sensitivity.

4. Interferometric Methods of Analysis in the Anomalous Dispersion Region

It is known that traditional interferometric methods of analysis are not selective, except for that the refractive index of the analyte is much higher than that of the interfering components. However, the selectivity of the analysis can be achieved when working in the anomalous dispersion region of the analyte [10]. Indeed, the frequency dependence of the refractive index near the absorption line center ω_0 has the form

$$N = 1 + \frac{k\mu}{\mu^2 + \gamma^2/4}, \tag{6}$$

where k is a constant depending on the analyte parameters, and $\mu = \omega - \omega_0$ is the frequency deviation from the center of the absorption line.

Hence, the refractive index is an odd function of the detuning and has a dispersion character (Fig. 2). The refractive indices in the maximum and minimum of this curve can differ significantly (by 10–20% in the case of strong absorption lines). Therefore, the displacement of the interference fringes of the working pattern will be proportional to the path difference, if the comparison cuvette is filled with clean air,

$$\Delta p = L(n_{\max} - n_p)X = k\lambda_p,$$

where λ_p and $n_{\max}$ are the wavelength and the refractive index, respectively, at the maximum of the dispersion curve; L is the length of the interferometer working chamber; n_p is the refractive index of air; and $k = 1, 2, 3, \ldots$. The shift of the reference interference pattern will be proportional to

$$\Delta p = L(n_p - n_{\min})X = k\lambda_0,$$

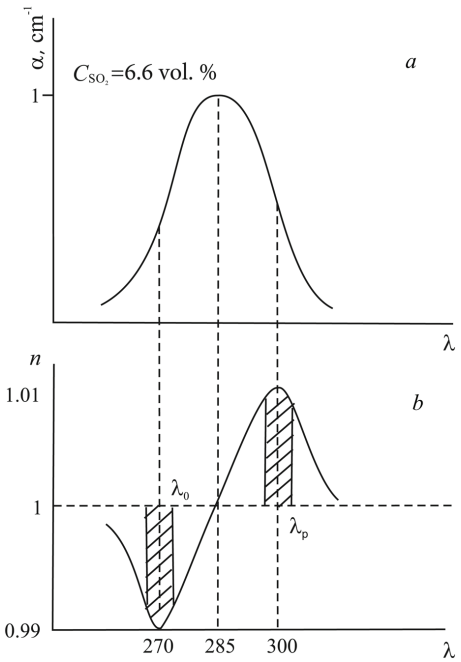

Fig. 2. Dependences of the absorption coefficient α (a) and the refractive index n (b) on the wavelength in the region of the SO_2 absorption band (a simplified view)

where λ_0 and $n_{\min}$ are the wavelength and the refractive index, respectively, in the dispersion curve minimum.

Let us consider a specific example. Suppose that we analyze SO_2 in the 285-nm region. The corresponding absorption coefficient $K \sim 40$ (cm atm)$^{-1}$. The wavelengths are $\lambda_p = 300$ nm and $\lambda_0 = 270$ nm. To extract those wavelengths, interference light filters 10 nm in width are used. The refractive index equals $n_{\max} = 1.1$ at λ_p, and $n_{\min} = 0.9$ at λ_0. Then, for the interference pattern to shift by half a fringe at $L = 10$ mm, the SO_2 concentration $X = 39 \times 10^{-6}$ is required. The initial interference pattern is shifted by 0.5 times half a fringe in the opposite direction at the SO_2 concentration $X = 33 \times 10^{-6}$. Therefore, if the cuvette length is 10 mm, the interval of SO_2 measurements will be equal to 0–25 ppm (to exclude a transition onto the second half-fringe).

Suppose that there is an interfering component in the gas mixture, e.g., CO_2, with a concentration that is 100 times higher than the measurement range. Then, the additional path difference induced by the presence of 0.25 vol% CO_2 equals $\Delta = 8 \times \times 10^{-6}$. Such a path difference corresponds to a SO_2

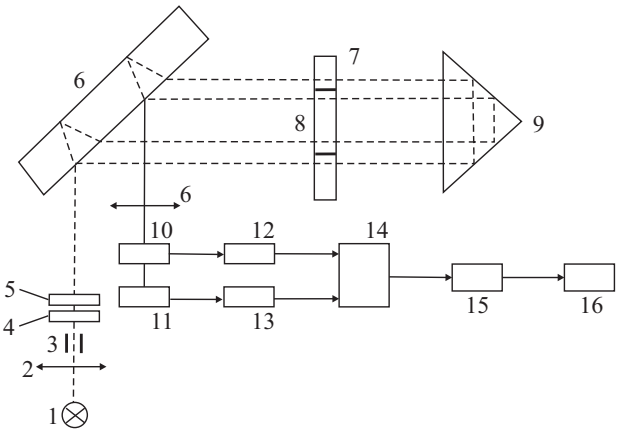

Fig. 3. Selective analyzer on the basis of a Jamin interferometer

concentration of 4×10^{-6}. However, the working and reference patterns are shifted in the same direction, i.e. the shift difference will be zero. Thus, the method guarantees the analysis selectivity $S_{\mathrm{m}}/S_{\mathrm{i}} \sim 10^5$, where S_m is a sensitivity to the measured component, and S_i to the interfering one. In addition, it significantly increases the sensitivity (by 2–3 orders of magnitude). Therefore, the devices based on this method can be used to analyze microconcentrations of the test gas in a multicomponent gas mixture.

In Fig. 3, *a*, a possible schematic diagram of a similar analyzer is depicted [11]. Radiation from lamp *1* is collimated by lens *2* and directed to diaphragm *3*, which separates the lower and upper parts of the light flux. Then, the upper part of the light flux is passed through light filter *4* in the working channel, the maximum transmittance of which corresponds to the dispersion curve maximum (Fig. 2), and the lower part of the light flux is passed through light filter *5* located beneath in the reference channel, which corresponds to the dispersion curve minimum. Each part of the light flux corresponding to two wavelengths is divided into two rays at light-dividing plate *6*. One of the rays of each wavelength passes through cuvette *7*, which contains the sample substance (e.g., the solvent) and through cuvette *8* containing the analyte. Then, the rays are reflected from prism *9* and pass through the same cuvettes again. Due to the difference between the refractive indices of the solvent and the analyte at two wavelengths, there arises a path difference.

At light-dividing plate *6*, the rays are mixed, and there emerge two interference patterns from the rays that have passed through the corresponding filters. It is clear that the fringe shifts with respect to the corresponding photodetectors *11* and *12* will have different signs for those interfering rays, say, the fringes of the working pattern will be shifted to the right, and those of the reference pattern to the left. With the help of lens *10*, those interference patterns are projected on the corresponding position-sensitive photodetectors *11* and *12* (a chip of the K849PP1 type), so that the width of the interference maxima or minima was of the same order of magnitude as the sizes of the light-sensitive areas of photodetectors. Then, when the fringes of the interference pattern are shifted, electrical signals with different polarities are registered at photodetectors *11* and *12* (the biases take place in different directions). They are amplified in amplifier *13* and directed to summator *14* and afterward to registration system *15*, which performs mathematical operations with this final signal according to a corresponding program. The result of the signal processing is directed to digital indicator *16* and exhibited in the concentration units of the analyzed component.

Concentration measurements of Hg vapor at the transition 6^3P_2-7^3S_1 with a wavelength of 546.1 nm [10] were performed experimentally. A sensitivity of 0.08 mg/m^3 was achieved.

5. Application of Phase Methods in Nonlinear Absorption Spectroscopy

Let us consider the application of phase methods in nonlinear absorption spectroscopy by the example of the ring gas laser (RGL). In the lasers of this type, the counter-propagating waves belonging to the same mode are independent and spatially separated. For this reason, their interference can be observed in an external interferometer. The interference pattern consists of a series of light and dark fringes, i.e. the interference maxima and minima. If the frequencies of the counter-propagating waves coincide, the interference pattern turns out fixed with respect to the photodetector. But if the frequencies are different, the pattern begins to "run" to the left or right depending on the sign of the frequency difference $f_1 - f_2$. As a result of passing by dark and light fringes over the photodetector sensitive layer, a beating signal is registered.

In the case of single-mode RGL, the dependence of the beating frequency of the counter-propagating

waves on the laser parameters is described by the expression [12]

$$f_{1,2} = \frac{\omega d b \delta \eta}{\alpha - \beta + (3/4)\theta\eta} - \\ - \left[m_1 \cos(\Phi + \vartheta_1) - m_2 \cos(\Phi + \vartheta_2)\right]/2, \quad (7)$$

where $m_{1,2}$ are the magnitudes and $\vartheta_{1,2}$ are the phases of the coupling coefficients for the counter-propagating waves; $b = \tau - \rho$; τ and ρ are the coefficients of frequency pulling by the own field and the field of counter-propagating wave, respectively; $\mu = \omega_0^{(+)} - \omega$ are odd functions of the frequency detuning; $\alpha - \beta + (3/4)\theta\eta$ is an even detuning function; α and β are the saturation coefficients by the own field and the field of counter-propagating wave, respectively; the parameter θ determines the degree of mode interaction; η is the excess of pumping over the threshold level; $\delta = (\eta_1 - \eta_2)/(\eta_1 + \eta_2)$ is the relative difference between the quality factors of the counter-propagating waves; and ω_d is a parameter that coincides with the resonator bandwidth, if the pumping insignificantly exceeds the threshold.

From expression (7), it follows that the beat frequency is maximum, if

$$\alpha - \beta + (3/4)\theta\eta = 0, \quad (8)$$

i.e. near the single-wave generation zone. The width of this zone is determined by condition (8). The beat frequency decreases with the deviation from the gain line center. Since the denominator in expression (6) increases with the pumping level, the beat frequency decreases. The pressure growth in the active medium leads to a decrease of the denominator and, hence, to an increase of the beat frequency.

If the 1 : 1 mixture of ^{20}Ne and ^{22}Ne isotopes is used, the quantity $\alpha - \beta + (3/4)\theta\eta \sim 1/2$ and does not depend on the detuning (the zone of single-wave generation does not appear). Then, expression (7) is an odd function of the detuning ($f_{1,2} \sim \mu$), and the beats exist along the whole gain circuit, passing through zero at the line center. As one can see, the dependence on the detuning has a dispersion character.

The experimental study of the beats of counter-propagating waves was performed on an experimental setup consisting (see Fig. 4) of mirror ring He–Ne laser *1* ($\lambda = 3.39$ μm) with an absorbing methane cell in its resonator. The resonator length was $L = 75$ cm, the pressure in the He-Ne gas discharge tube was

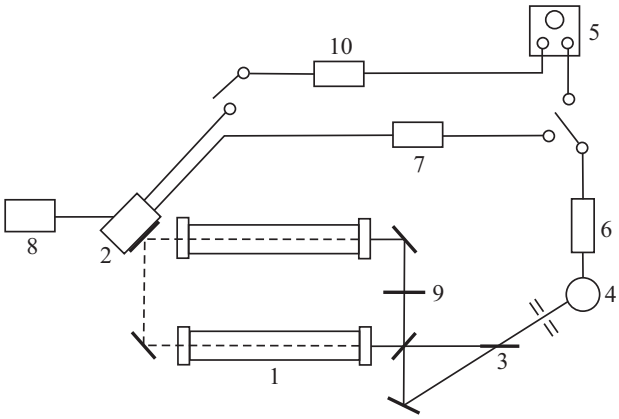

Fig. 4. Experimental setup to study the beats of counter-propagating waves in the ring gas laser (RGL) and its stabilization

200 Pa, and the pressure in the methane cell was 1 Pa. One of the resonator mirrors was mounted on piezoceramics *2*, which allowed the scanning of the resonator length when applying a saw-tooth voltage from generator *10* to piezoceramics and the change of the lasing frequency within the Doppler gain circuit using the controlled dc voltage source *8*. The counter-propagating waves of the ring laser were mixed in external interferometer *3*, and their beats (the interference pattern) were detected using photodetector *4*. The beat signal was observed on oscilloscope *5* (C1-31). In such a way, the dependence of the frequency of counter-wave beats on various parameters of the He–Ne laser (the pump level, the pressure of the active medium, the ratio of the active medium components ^{20}Ne and ^{22}Ne in He) was studied.

The dependences of the beat frequency on the detuning in the cases of one isotopic mixture (curve *1*) and a mixture of two isotopes (curve *2*) are shown in Fig. 5. The pressure of the active medium $P_{\mathrm{He-Ne}} = 200$ Pa, the pump level $\eta = 0.6$. The curves have a dispersion character and are odd functions of the detuning. The beat frequency also depends on the coupling coefficient of the counter-propagating waves (see below): the higher the coupling coefficient, the lower the beat frequency. Additionally, the character of the beat frequency dependence on the detuning also changes.

Figure 6 demonstrates the dependence of the weaker wave intensity, when scanning the lasing frequency (oscillogram (a)). The arrow marks the resonance induced by the methane absorption satura-

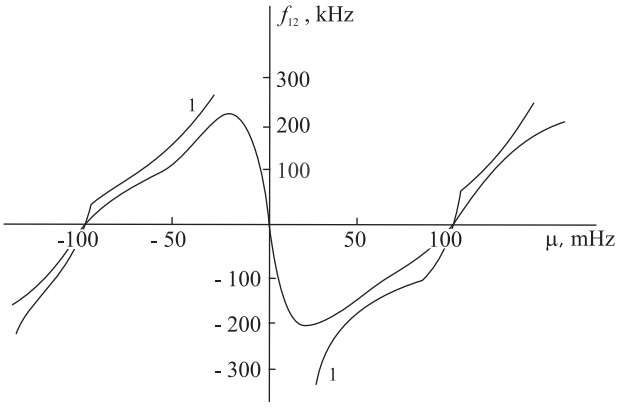

Fig. 5. Dependences of the beat frequencies of counter-propagating waves on the lasing frequency shift with respect to the center of the amplification line

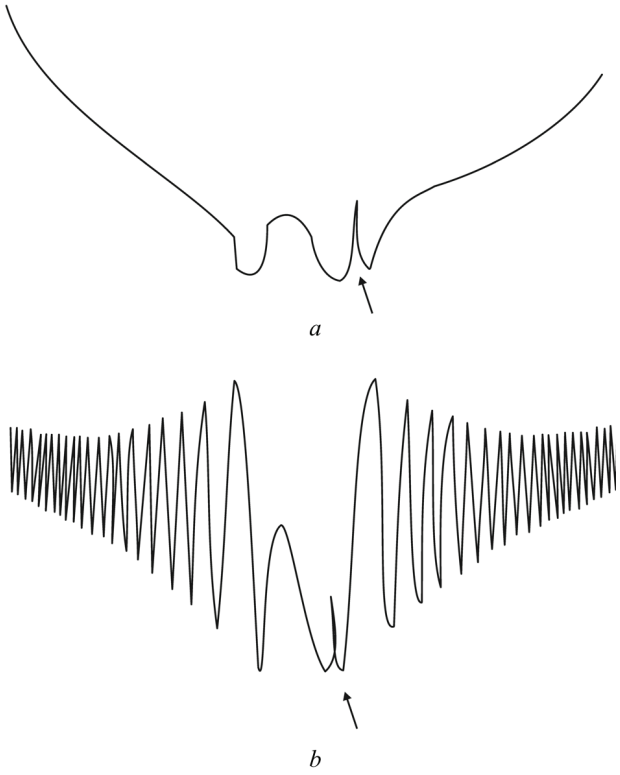

Fig. 6. Dependences of the weaker-wave intensity change (*a*) and the beat frequency of counter-propagating waves (*b*) on the laser generation frequency

tion. The resonance width is 100 kHz. The width of the neighbor resonance, which is a result of the synchronization of the counter-propagating waves at the amplification line center, is equal to 3 MHz. The pressure of the active medium is $P_{\mathrm{He-Ne}} = 200$ Pa. The lower oscillogram (*b*) was obtained for the waves shifted in the external interferometer. As one can see, when the RGL frequency approaches the zone of single-wave generation and the coupling of the counter-propagating waves is strong, the beat frequency first increases and then decreases, with the beat phase changing at the center. The dispersion dependence of the beat frequency on the detuning in the region of a methane resonance (marked by an arrow) can be obtained by changing the phase of the backward reflection coefficient of the stronger wave. Thus, the beating of the counter-propagating waves at the center of the amplification or absorption line changes the phase to the opposite one, and the dependence of the beat frequency on the detuning in this region has a form of dispersion curve.

Such a behavior of the counter-propagating wave beats near the center of the amplification or absorption line can be used to stabilize the RGL generation frequency [13].

When stabilizing the laser generation frequency with respect to the beats of its counter-propagating waves, the two-element photodetector FUL-611 is used as photodetector *4* (Fig. 4). A signal from photodetector *4* is amplified by differential amplifier *6* and is directed to dc amplifier *7*, which is connected to piezoceramics *2*. To adjust the frequency to the absorption line center (amplification), where the beating of counter-propagating waves is absent, since the latter are synchronized, a controlled dc voltage source 8 connected to piezoceramics *2* is used.

Thus, by changing the resonator length using dc voltage source *8*, the coincidence of the laser generation frequency with the center of the amplification (absorption) line and, thus, the break of the interference pattern motion with respect to photodetector *4* are achieved. In so doing, the same source *8* is applied to obtain a situation, when both light-sensitive elements of photodetector *4* are illuminated identically by the middle parts of the corresponding interference maximum wings. Usually, a multipolar power supply of photodetectors of this type is applied. Therefore, at the uniform illumination of its elements, the signal at the output of differential amplifier *6* equals zero, and when the interference pattern is shifted to the right or left with respect to the photodetector, there appears a constant signal of the corresponding polarity at the output of amplifier *6*. This signal is

amplified by dc amplifier *7* and directed to piezoceramics *2*, returning the interference pattern back to its original position.

Following this way, two RGLs were stabilized at the center of the amplification and absorption lines. The short-term frequency stability values were 2.6×10^{-11} and 5×10^{-12} per 1 s, respectively, when stabilizing at the center of the amplification or absorption line. The values of the long-term stability per 1 h amounted to 10^{-8} and 3×10^{-11} in those two cases.

As one can see, the application of the dependence of the phase difference between the counter-propagating waves on the detuning in order to stabilize the RGL generation frequency makes it possible to obtain a good short-term frequency stability without much difficulty, which is required in a number of applications, including the creation of analytical instruments as well.

Let us now consider how a phase-resonance stabilized RGL can be used for concentration measurements. In the RGL, the frequency shift associated with a change in the magnitude and phase of the coupling coefficients of the counter-propagating waves is very substantial. In particular, according to work [14], the RGL frequency shift equals

$$\Delta\Omega = (2\Gamma m_1/m_2)(I_2(0)/I)\sin(\vartheta_1 - \vartheta_2). \qquad (9)$$

Here, Γ is the resonance width, $I_2(0)$ the weak wave intensity at the resonance center, when the central resonance frequencies of the passive and active media coincide, $I = I_1 + I_2$ is the total intensity of counter-propagating waves, $m_{1,2} = 2c/L(1-R)\sqrt{R_{1,2}}$ are the absolute values of the coupling coefficients, R is the reflection coefficient of the mirror behind which additional mirrors with the reflection coefficients R_1 and R_2 are installed (they return some radiation to the resonator), and $\vartheta_{1,2}$ are the phases of the reflected strong and weak waves. The intensity of phase resonances, when measuring the phase difference $\Theta = \vartheta_1 - \vartheta_2$, is given by the expression [15] $I_2 = I_2(0)(1 - k\sin\Theta)$, where k is a coefficient that accounts for the presence of an internal connection between the counter-propagating waves in the laser resonator (scattering at mirrors, inhomogeneities of the active medium, and so forth). However, the magnitudes of the coefficients $(m_{1,2})_{\rm in} \ll (m_{1,2})_{\rm out}$, and the coefficient k are close to 1.

If the KGL is stabilized with respect to resonances 100 kHz in width, one mirror is installed outside the resonator, which returns and reflects the strong wave radiation into the laser resonator, i.e.

$$(m_1)_{\rm out} + (m_1)_{in} = m_1 \gg m_2 = (m_2)_{\rm in},$$

the resonance contrast $I_2(0)/I = 0.2$, and the phase difference $\Theta = 90^\circ$ (i.e. $\sin\Theta = 1$). Then, in accordance with Eq. (9), we obtain $\Delta\Omega = 400$ kHz. If the instability of the generation frequency equals ±10 kHz (this is quite a realistic value), the measurement error of the shift value will be 2.5×10^{-5}, which is two orders of magnitude better than when measuring photometric values(transmission or reflection).

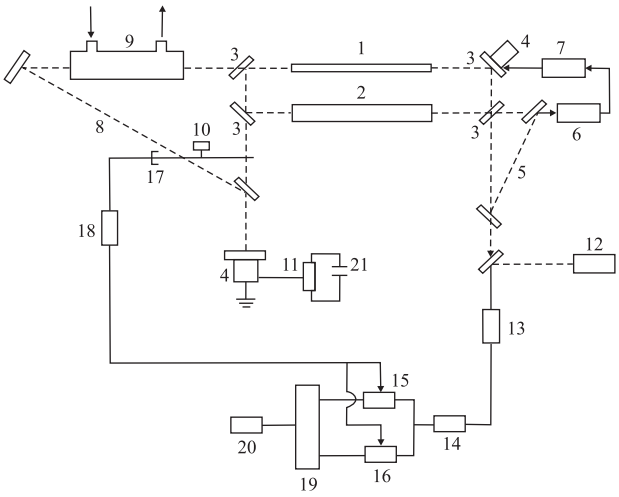

Fig. 7. Analyzer based on a frequency-stabilized RGL

Taking the aforesaid into account, one of the authors proposed to use, in concentration measurements, the frequency shifts of the frequency-stabilized ring He–Ne laser [16], which arise owing to a reduction of the reflection coefficient R of the mirror that returns radiation, when radiation is absorbed in the cuvette with the analyzed gas which is installed in front of this mirror, as well as owing to the phase change of reflected radiation as a result of the variation of its optical path in this cuvette. The idea of the method is explained in Fig. 7 [17].

Radiation of the RGL consisting of He–Ne gas discharge tube *1*, absorbing cell *2* filled with CH_4 at a pressure of 1 Torr, and four mirrors *3*, one of which is mounted on piezoelectric corrector *4*, enters external interferometer *5*, where the counter-propagating waves I_1 and I_2 are mixed. The beating of those waves is registered by means of photodetector *6* with two

sites of the FUL-611 type. AFC system *7* processes the deviation of the laser generation frequency from the center of the amplification or absorption line. In this case, the corrective AFC voltage is supplied to piezoelectric corrector *4*. Mixer *8*, where the radiation of the stronger wave that comes out through different mirrors from the RGL is directed to, contains cuvette *9* through which the analyzed gas mixture is pumped. Modulator *10* alternately blocks the radiation passed through cuvette *9* and the radiation that is directed past it. The light flux coming out from mixer *8* is reflected from mirror *11* mounted on piezoelectric corrector *4* and re-enters the laser resonator through cuvette *9* or past it depending on the position of the disk of modulator *10*. Radiation that has passed twice through cuvette *9* twice

• is absorbed by the analyzed gas (for example, CH_4) presenting in the sample, which reduces the magnitude of the coupling coefficient of counter-propagating waves to the value $m_1' = m_1 \exp(-XKL)$;

• undergoes the phase change of the reflected wave by $\Delta\vartheta_1 = 2\pi/\lambda(n_{CH_4} - n_r)XL$.

Let us consider the case where the concentration of CH_4 in the cuvette is equal to $X = 10^{-6}$. The cuvette length is 100 mm, the other parameters were indicated above. Then, in accordance with Eq. (9), a new value of the shift due to a change in the magnitude of the wave coupling coefficient will be $\Delta\Omega - \Delta\Omega' = 0.76$ kHz. It is difficult to evaluate $\Delta\vartheta_1$ because of the lack of data on a change of the CH_4 refractive index in this narrow spectral interval in the case of absorption saturation. However, we may expect that a change of the reflected wave phase will have a stronger (several orders of magnitude) effect on the frequency shift than on the decrease of the shear modulus of the counter-propagating waves.

To register a change in the RGL radiation frequency shift, radiation was mixed with radiation of another frequency-stabilized laser *12*. The frequency of their beats is registered by photodetector *13* with a small time constant, amplified in broadband amplifier *14* and supplied to counters *15* and *16* of the working and reference channels. The counters are triggered by pulses coming from the position sensor of modulator *17* through former *18*. In the counter of reference channel *16*, the frequency shift is fixed at such a position of modulator *10*, when laser radiation does not pass through cuvette *9*; in counter *15* of the working channel, the frequency shift is fixed taking radiation absorption in cuvette *9* into account. In register system *19*, the frequency signals are processed according to a certain algorithm (for example, $(\Delta\Omega - \Delta\Omega')/\Delta\Omega$), and the measurement result is demonstrated on indicator *20*.

As one can see, the frequency change in the presence of the analyzed component in cuvette *9* is rather large even at low concentrations of the analyte (a CH_4 concentration of 10^{-6} corresponds to the background concentration of methane in atmospheric air) and if only the change of $m_{1,2}$ moduli is taken into account.

6. Conclusions

As we can see, the transition to the frequency shift measurement (instead of the direct transmittance measurement) significantly increases the measurement accuracy and sensitivity (at an absolute instability of the RGL generation frequency of 10 Hz, the measurement accuracy is 10^{-6}). The presence of the phase component of the useful signal, which in the region of anomalous dispersion of the analyte is several orders of magnitude larger than the amplitude component and linearly depends on the concentration, allows measurements to be performed in a wide interval of the analyzed component concentrations. Therefore, the use of the phase component of the useful signal (see Eq. (4)) is more desirable, because it makes it possible to achieve high values for the selectivity and analysis accuracy, and to simplify the calibration and verification [18].

Of course, the choice of that or another measurement method depends on the experience and qualification of the experimenters, the presence of an appropriate equipment, and so on. Therefore, it is impossible to say unequivocally which of the methods and how much is better.

The proposed methods of analysis are not a panacea for all problems. The choice of a specific method of analysis depends on many factors, and, in the area where standard methods do not work, there are alternative methods proposed by the authors.

1. R.H. Wiens, H.H. Zwick. *Infrared, Correlation, and Fourier Transform Spectroscopy.* Edited by J.S. Mattson, H.B. Mark, jr., H.C. MacDonald, jr. (Marcel Dekker, 1977).
2. T.V. Ward, H.H. Zwick. Gas cell correlation spectrometer: GASPEC. *Appl. Opt.* **14**, 2896 (1975).

3. V.R. Kozubovskii. *Devices and Methods of Optical Absorption Control over Atmospheric Air Pollution Based on Selective Filtration.* Dr.Sci. thesis (MIKhM, Moscow, 1991) (in Russian).
4. W. Demtröder. *Laser Spectroscopy* (Springer, 2002).
5. W.C. Marlow. Hakenmethode. *Appl. Opt.* **6**, 1715 (1967).
6. N.I. Bogdanskis, V.S. Bukreev, G.N. Zhizhin, M.N. Popov. *Modern Trends in Spectroscopy Technique* (Nauka, 1982) (in Russian).
7. T. Okamoto, S. Kawata. A photodiode array Fourier transform spectrometer based on a birefringent interferometer. *Appl. Spectrosc.* **40**, 691 (1986).
8. *Ultrasensitive Laser Spectroscopy.* Edited by D.S. Kliger (Academic, 1983)
9. V.R. Kozubovskii. Inventor's certificate 1805746 USSR, MKI G01N 21/61.
10. V.R. Kozubovskii, A.A. Bulyga. Method for increasing the sensitivity and selectivity of interferometric gas analyzers. *Zh. Prikl. Spektrosk.* **55**, 300 (1991) (in Russian).
11. V.R. Kozubovskii. Inventor's certificate 1608990 USSR, MKI G01N 21/45.
12. Yu.L. Klimontovich. *Statistical Theory of Open Systems. Vol. 1: A Unified Approach to Kinetic Description of Processes in Active System* (Springer, 1995).
13. V.R. Kozubovskii. Stabilization of the frequency of a ring gas laser by the beats of its counter-propagating waves. *Zh. Prikl. Spektrosk.* **49**, 903 (1988) (in Russian).
14. M.V. Danileiko, A.M. Fal, V.P. Fedin, M.T. Shpak, L.P. Yatsenko. Frequency reproducibility of ring He–Ne/CH_4 lasers. *Kvant. Electron.* **9**, 2013 (1982) (in Russian).
15. M.V. Danileiko, V.R. Kozubovskii, V.P. Fedin, M.T. Shpak. *Study of Power Resonances of the Ring Laser.* Preprint No. 9 (Institute of Physics of the Academy of Sciences of the Ukrainian SSR, Kyiv, 1977) (in Russian).
16. V.R. Kozubovskii. Gas analyzer based on a frequency-stabilized ring laser. *Zh. Prikl. Spektrosk.* **58**, 355 (1993) (in Russian).
17. V.R. Kozubovskii. Inventor's certificate 1811287 USSR, MKI G01N 21/61, 21/39.
18. V.R. Kozubovskii. Patent of invention No. 100559 UA, MPK G01N 21/61, 2013, Bull. No. 1.

Received 30.08.20.
Translated from Ukrainian by O.I. Voitenko

В. Козубовський, Ю. Білак

ФАЗОВІ МЕТОДИ
В АБСОРБЦІЙНІЙ СПЕКТРОСКОПІЇ

Аналіз газового складу повітря є актуальною задачею, оскільки від його якості залежить самопочуття і здоров'я людини. Більшість методів аналізу газового середовища є недосконалими, часто відсутні необхідні чутливість, селективність і точність. Стаття присвячена аналізу можливості оптимізації селективності і точності інтерферометричних (рефрактометричних) приладів газового аналізу. Основна ідея роботи полягає у демонстрації можливості переходу від безпосереднього вимірювання відношення інтенсивностей світлових потоків до вимірювання частотних зсувів та частоти випромінювання, що суттєво підвищує точність і чутливість вимірювань. Для підвищення ж селективності аналізу авторами роботи пропонується проводити вимірювання в області аномальної дисперсії аналізованого газового компонента. Наявність фазової складової корисного сигналу, яка в області аномальної дисперсії на декілька порядків більше амплітудної складової і лінійно залежить від величини концентрації, дозволяє проводити вимірювання в широкому діапазоні концентрацій аналізованого компонента. Все це відкриває нові можливості для інтерферометричних методів газового аналізу.

Ключові слова: інтерферометр, аномальна дисперсія, кільцевий газовий лазер, газоаналізатор, абсорбційна спектроскопія.